Cell Host & Microbe
Article

Matrix Protein 2 of Influenza A Virus Blocks Autophagosome Fusion with Lysosomes

Monique Gannagé,[1,2,8] Dorothee Dormann,[2,8] Randy Albrecht,[3] Jörn Dengjel,[6,9] Tania Torossi,[1] Patrick C. Rämer,[1] Monica Lee,[2] Till Strowig,[2] Frida Arrey,[2] Gina Conenello,[3,6] Marc Pypaert,[7] Jens Andersen,[6] Adolfo García-Sastre,[3,4,5] and Christian Münz[1,2,*]

[1]Viral Immunobiology, Institute of Experimental Immunology, University Hospital of Zürich, 8057 Zürich, Switzerland
[2]Laboratory of Viral Immunobiology and Christopher H. Browne Center for Immunology and Immune Diseases, The Rockefeller University, New York, NY 10065, USA
[3]Department of Microbiology
[4]Department of Medicine, Division of Infectious Diseases
[5]Global Health and Emerging Pathogens Institute
Mount Sinai School of Medicine, New York, NY 10029, USA
[6]Center of Experimental BioInformatics, Department of Biochemistry and Molecular Biology, University of Southern Denmark, 5230 Odense, Denmark
[7]Department of Cell Biology, Yale University School of Medicine, New Haven, CT 06520, USA
[8]These authors contributed equally to this work
[9]Present address: School of Life Sciences - LIFENET, Freiburg Institute for Advanced Studies (FRIAS), Albertstr. 19, 79104 Freiburg, Germany
*Correspondence: christian.muenz@usz.ch
DOI 10.1016/j.chom.2009.09.005

SUMMARY

Influenza A virus is an important human pathogen causing significant morbidity and mortality every year and threatening the human population with epidemics and pandemics. Therefore, it is important to understand the biology of this virus to develop strategies to control its pathogenicity. Here, we demonstrate that influenza A virus inhibits macroautophagy, a cellular process known to be manipulated by diverse pathogens. Influenza A virus infection causes accumulation of autophagosomes by blocking their fusion with lysosomes, and one viral protein, matrix protein 2, is necessary and sufficient for this inhibition of autophagosome degradation. Macroautophagy inhibition by matrix protein 2 compromises survival of influenza virus-infected cells but does not influence viral replication. We propose that influenza A virus, which also encodes proapoptotic proteins, is able to determine the death of its host cell by inducing apoptosis and also by blocking macroautophagy.

INTRODUCTION

Influenza virus is a segmented negative-sense RNA virus. The eight RNA segments of influenza A viruses encode 11 proteins (Palese and Shaw, 2007). The three largest segments are dedicated to produce each of the three RNA polymerase components, and one of them encodes an additional polypeptide, polymerase basic protein 1-frame 2 (PB1-F2), which promotes cell death (Chen et al., 2001). Two of the segments encode the surface glycoproteins hemagglutinin (HA) and neuraminidase (NA), involved in sialic acid adhesion and fusion in endosomes. One segment encodes the nucleoprotein (NP) involved in viral RNA packaging and transport and one the two matrix proteins (M1 and M2). M2 possesses proton channel activity that allows virion acidification for efficient uncoating after fusion in endosomes. On top of these mostly structural proteins encoding RNA segments, the smallest segment encodes the nonstructural proteins NS1 and NS2. NS2 or NEP supports the nuclear export of viral RNA packaged with NP. NS1 compromises the interferon (IFN) response to viral infection by multiple mechanisms, including binding to double-stranded RNAs and preventing their recognition by the innate immune system. Although many aspects of influenza virus pathogenesis have been investigated, a more detailed understanding of the virus-host interaction, especially infection-induced changes in the biology of the host cell, could reveal critical points of the influenza virus life cycle that could be targeted to cripple virus replication and diminish virus production. This is especially important because the virus causes significant morbidity and mortality even outside pandemics. Influenza virus infection is associated with 20,000 deaths in the US in a typical year and causes, in addition, significant losses in the tens of billions of US dollars to the economy due to debilitating infections (Yewdell and García-Sastre, 2002). Even more dramatically, the virus causes periodic pandemics with a higher death toll. Therefore, it is important to characterize additional control mechanisms and the virus' countermeasures against them.

One such control mechanism could be macroautophagy, and indeed, many pathogens have been found to interfere with this catabolic process (Schmid and Münz, 2007). Autophagic and proteasomal degradation are the two main catabolic processes for proteins in eukaryotic cells. While the proteasome discards primarily short-lived soluble ubiquitinated proteins (Ciechanover, 2005), autophagy is thought to degrade cellular organelles and protein aggregates of primarily long-lived proteins (Mizushima and Klionsky, 2007). Autophagy consists of at least three pathways: microautophagy, macroautophagy, and chaperone-mediated autophagy. Of those, macroautophagy is best characterized and has been implicated in both innate and adaptive

immunity (Schmid and Münz, 2007). During macroautophagy, an isolation membrane forms around its substrate to generate an autophagic vesicle surrounded by two membranes. This autophagosome then fuses with late endosomes and lysosomes to degrade the inner autophagosome membrane and the autophagic cargo. More than 30 essential autophagy genes (*atg*) have been identified in yeast for this process (Mizushima and Klionsky, 2007). While the function of most of these is still unknown, two ubiquitin-like systems have been characterized as essential for autophagosome generation (Ohsumi, 2001). In one of them, Atg12 is coupled to Atg5, which then, in complex with Atg16L1, decorates the outer membrane of the isolation membrane. Upon autophagosome completion, this complex is recycled. The Atg12/Atg5/Atg16L1 complex is essential for autophagosome formation and might influence the curvature of the forming autophagosome as well as guide coupling of Atg8/LC3, the second ubiquitin-like molecule involved in macroautophagy (Hanada et al., 2007; Fujita et al., 2008). This second ubiquitin-like system couples Atg8/LC3 to phosphatidylethanolamine at the outer and inner autophagosomal membrane. Atg8/LC3 stays with the completed autophagosome and is in part degraded with the inner vesicle membrane by lysosomal hydrolysis. These ubiquitin-like conjugation reactions are initiated by class III phosphatidylinositol 3-kinase (PI3K) complexes, which include the Atg6/Beclin-1 protein. Interestingly, Atg6/Beclin-1-positive complexes that contain Atg14L seem to support autophagosome formation, while others that contain UVRAG may facilitate the fusion between autophagosomes and lysosomes (Matsunaga et al., 2009; Zhong et al., 2009; Itakura et al., 2008).

This knowledge of the molecular mechanisms of autophagosome generation allowed us to analyze macroautophagy regulation by influenza virus infection. We found that influenza A virus infection arrests autophagosome degradation in large perinuclear structures. We could identify influenza A M2 as sufficient and required for this phenotype, compromising macroautophagy, which is required for the survival of the infected host cells. Therefore, we propose that influenza A virus has at least two mechanisms to regulate cell death of its host cell: PB1-F2 inducing apoptosis and M2 inhibiting antiapoptotic macroautophagy.

RESULTS

Autophagosomes Accumulate after Influenza Virus Infection

In order to investigate whether the cellular macroautophagy level is altered in response to influenza A virus infection, we infected stably GFP-LC3-transfected human epithelial cell lines with influenza virus strain A/Aichi/68 (H3N2). Cells were infected at a low multiplicity of infection (moi between 0.6 and 0.8), which typically resulted in an infection rate of 50%–70% (data not shown). At these mois, cell viability was maintained at 90% 24 hr postinfection, whereas 48 hr postinfection, up to 50% of apoptotic cells could be detected (data not shown). We therefore chose to analyze cells 24 hr postinfection. In comparison to uninfected cells, influenza-infected cells showed a strong increase in GFP-LC3$^+$ autophagosomes (Figure 1A). Autophagosome accumulation was observed in A549 human lung epithelial cells, MLE-12 mouse lung epithelial cells, MDAMC human breast carcinoma cells, and HaCat human keratinocyte cells (Figure 1A). The increase in autophagosomes in A549 human lung epithelial cells occurred after infection with different strains of influenza virus (A/Aichi/68 [H3N2], A/WSN/33 [H1N1], and A/PR8/34 [H1N1]) (Figure 1B). The increased autophagosome number could also be observed by western blot at the level of endogenous lipidated Atg8/LC3 (Figure 1C). When lysates of uninfected and infected cells were analyzed by anti-Atg8/LC3 immunoblot, the lipidated and therefore faster-migrating Atg8/LC3-II form was strongly increased in influenza-infected epithelial cell lines (Figure 1C). In addition to Atg8/LC3 as an autophagosome marker, we also analyzed accumulation of previously described autophagosome cargo (Klionsky et al., 2008). Both polyubiquitinated protein aggregates and p62/sequestosome 1 (SQSTM1), previously described macroautophagy substrates (Komatsu et al., 2006; Hara et al., 2006; Bjørkøy et al., 2005; Pankiv et al., 2007), accumulated in autophagosomes upon influenza infection (Figures 1D and 1E). These data demonstrate that autophagosomes accumulate after epithelial infection with influenza A virus, suggesting that macroautophagy is a process that is regulated during influenza virus infection.

Live Influenza Virus Infection Is Required for Autophagosome Accumulation

To investigate how long after infection the autophagosome increase occurs, we prepared lysates at various time points postinfection and analyzed them by anti-Atg8/LC3 western blot. Atg8/LC3-II was first detectably increased 10 hr after infection of lung epithelial cells and gradually accumulated to higher levels at later time points (Figure S1A). Thus, the autophagosome accumulation was not a rapid response to influenza virus infection, suggesting that viral or cellular factors might have to be produced first.

To see whether cells have to be productively infected or whether uptake of inactivated viral particles and perhaps recognition of pathogen-associated molecular patterns (PAMPs) within these is sufficient to mediate autophagosome accumulation, we exposed cells to live or heat-inactivated influenza A virus and analyzed their lipidated Atg8/LC3-II levels by western blot analysis (Figure S1B) and autophagosome content by GFP-Atg8/LC3 fluorescence microscopy (Figure S1C). Only live influenza virus was able to elicit an increase of autophagosomes as indicated by GFP-Atg8/LC3-II, endogenous Atg8/LC3-II, and GFP-Atg8/LC3 vesicle accumulation, whereas heat-inactivated virus did not cause any change in Atg8/LC3-II levels or GFP-Atg8/LC3 distribution (Figures S1B and S1C). Thus, contact with the components or endocytosis of inactivated virus particles is not sufficient to elicit autophagosome accumulation.

To visualize more directly that productive infection is necessary for macroautophagy regulation, we stained uninfected and infected cells with M1-specific antibodies to see if the autophagosome accumulation would only occur in cells that produce viral protein. Indeed, autophagosome accumulation and formation of large perinuclear autophagosomes were only detectable in cells that expressed influenza A M1, whereas M1-negative cells did not show these changes in intracellular GFP-Atg8/LC3 distribution (Figure S1D). This indicates that autophagosome

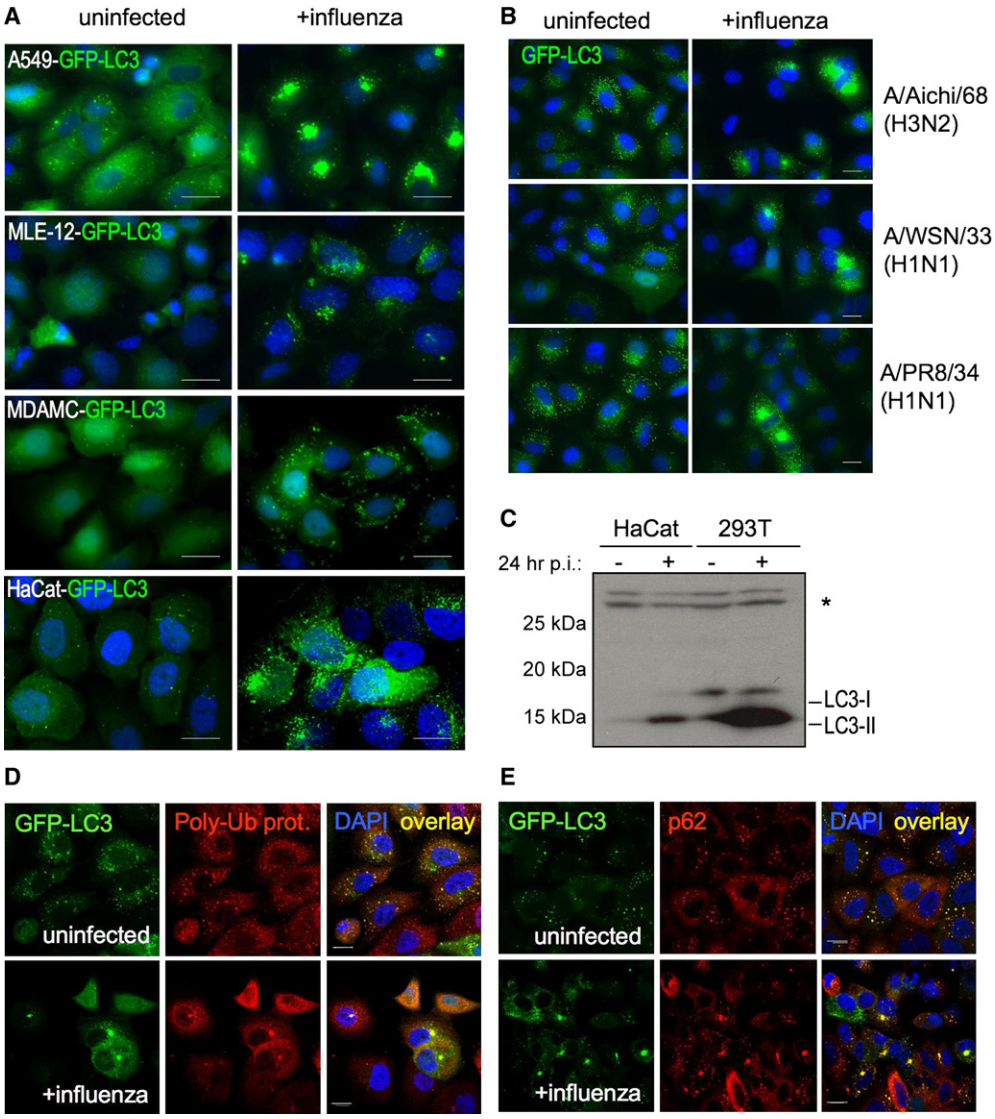

Figure 1. Classical Autophagosome Accumulation after Influenza A Virus Infection

(A) Stably GFP-Atg8/LC3-transfected epithelial cell lines A549, MLE-12, MDAMC, and HaCat were infected with influenza A/Aichi/68 virus and analyzed for GFP-Atg8/LC3-positive autophagosome accumulation 24 hr later by fluorescence microscopy. DAPI was used to stain nuclear DNA. Scale bar: 30 μm.

(B) GFP-Atg8/LC3-transfected A549 human lung epithelial cells were infected with different influenza A virus strains (A/Aichi/68, A/WSN/33, and A/PR8/34) and analyzed after 24 hr. One of three experiments is shown. Scale bar: 30 μm.

(C) The human epithelial cell lines HaCat and 293T were infected with influenza A/Aichi/68 virus at an moi of 0.1. Twenty-four hours postinfection, lysates of uninfected and infected cells were analyzed by western blot analysis for Atg8/LC3. Unconjugated (LC3-I) and lipidated Atg8/LC3 (LC3-II) can be distinguished by their apparent molecular weights of 18 kDa and 16 kDa, respectively. * marks an unspecific band, detected by our Atg8/LC3 antiserum. One of three experiments is shown.

(D and E) Twenty-four hours after influenza A virus infection, colocalization of GFP-ATG8/LC3 and the classical macroautophagy substrates polyubiquitinated proteins (D) and p62/SQSTM1 (E) were analyzed by immune fluorescence microscopy. Nuclear DNA was stained with DAPI. Scale bar: 20 μm. One of three experiments is shown.

accumulation occurs only in directly and productively infected cells and is not mediated by a soluble factor secreted in response to influenza virus infection. In line with these observations, we could rule out that type I IFNs were responsible for the observed effect, because blocking of the IFNα/β receptor did not abrogate the influenza-mediated autophagosome accumulation (data not shown). Therefore, productive influenza A infection causes autophagosome accumulation.

Influenza Virus Infection Blocks Autophagosome Degradation

Since autophagosomes are transient vesicles that deliver their cargo within minutes for lysosomal hydrolysis, their accumulation could result from increased formation or decreased degradation (Klionsky et al., 2008). To investigate which of these two mechanisms was responsible for autophagosome accumulation upon influenza virus infection and if fusion of autophagosome

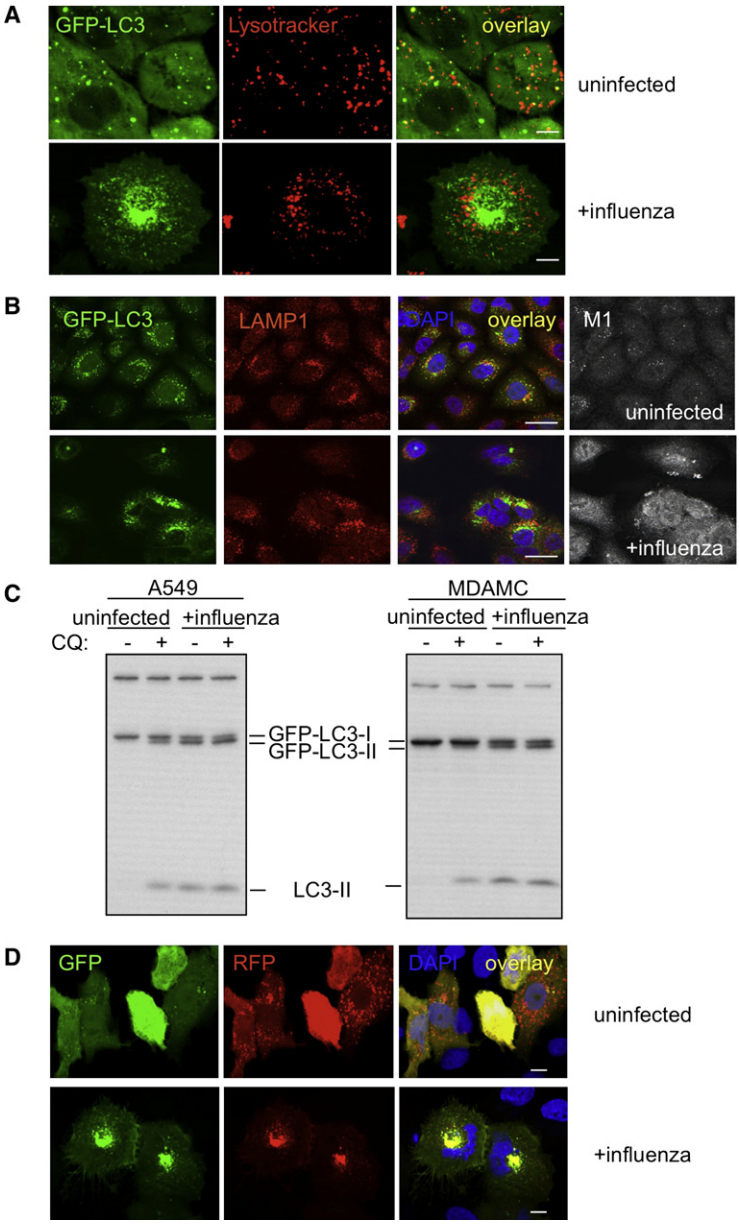

Figure 2. Autophagosomes Do Not Fuse with Acidified Proteolytic Lysosomes in Influenza-Infected Cells

(A) Live cell imaging was performed to analyze colocalization of LysoTracker-stained acidified vesicles and GFP-Atg8/LC3-positive autophagosomes in uninfected and influenza A virus-infected cells. Scale bar: 15 μm. Representative still images of two independent experiments are shown.

(B) Furthermore, fusion of autophagosomes with lysosomes was analyzed as colocalization of the autophagosome marker GFP-Atg8/LC3 with the lysosome marker LAMP1. Nuclear DNA was stained with DAPI and infected cells with M1-specific antibodies. Scale bar: 30 μm. One of three experiments is shown.

(C) GFP-Atg8/LC3-transfected A549 human lung epithelial and MDAMC human breast carcinoma cells were infected with influenza A virus at an moi of 0.4 for 24 hr. Then the indicated samples were treated for 6 hr with the lysosomal inhibitor chloroquine (CQ), and lipidated endogenous Atg8/LC3-II and lipidated transfected GFP-Atg8/LC3-II content was analyzed by Atg8/LC3-specific western blot analysis. One of three experiments is shown.

(D) The tandem reporter construct mRFP-GFP-Atg8/LC3 was transiently transfected into uninfected or influenza A virus-infected A549 human lung epithelial cells. GFP (sensitive to acidification and lysosomal degradation) and RFP (insensitive to acidification and lysosomal degradation) fluorescence of the reporter construct were analyzed by fluorescence microscopy. DAPI was used to stain nuclear DNA. Scale bar: 20 μm. One of three experiments is shown.

with lysosomes was intact in infected cells, we labeled acidic compartments with red fluorescent LysoTracker and performed live cell imaging (Figure 2A). In uninfected cells, about 25% of GFP-Atg8/LC3$^+$ vesicles overlapped with LysoTracker staining, indicating that a fraction of autophagosomes had fused with lysosomes and had become acidified. In contrast, in influenza-infected cells, almost no overlap between autophagosomes and LysoTracker staining was observed; especially the large perinuclear autophagosomes were devoid of LysoTracker staining (Figure 2A). This suggests that, after influenza virus infection, autophagosomes do not fuse with acidic compartments; even so, acidified lysosomes were present at similar numbers in infected cells. In order to rule out that autophagosomes fuse with lysosomes but are not efficiently acidified in infected cells, we investigated GFP-Atg8/LC3 colocalization with the lysosome-associated membrane protein 1 (LAMP1) (Figure 2B). While GFP-Atg8/LC3 partially overlapped with LAMP1 in uninfected lung epithelial cells, this autophagosome marker did not colocalize with LAMP1 in influenza virus-infected cells. Especially, the large GFP-Atg8/LC3-positive perinuclear vesicles were LAMP1-negative. These data suggested that autophagosomes do not efficiently fuse with lysosomes in influenza-infected cells.

In order to confirm this block of autophagosome fusion with lysosomes in influenza virus-infected cells, we analyzed the turnover of autophagosomes. For this purpose, influenza virus-infected and mock-infected cells were treated, 24 hr postinfection, with the lysosomal proteolysis inhibitor chloroquine (CQ) for 6 hr. In uninfected cells, lipidated Atg8/LC3-II and GFP-Atg8/LC3-II accumulated upon CQ treatment, indicating that autophagosomes are turned over by lysosomal proteolysis (Figure 2C). In contrast, in influenza-infected cells, no further accumulation of Atg8/LC3-II and GFP-Atg8/LC3-II could be observed in response to CQ treatment, demonstrating that autophagosomes were not turned over at a significant rate by lysosomal proteolysis in infected cells. As a second indication that lysosomal turnover of autophagosomes is defective in influenza virus-infected cells, we made use of a tandem reporter construct, mRFP-GFP-Atg8/LC3 (Kimura et al., 2007). The GFP moiety of this tandem autophagosome marker is sensitive to lysosomal proteolysis and quenching in acidic pH, while the mRFP is not. Therefore, the green fluorescent component of the composite yellow fluorescence for this mRFP-GFP-LC3 reporter is lost upon autophagosome fusion with lysosomes. This fluorescence change from yellow to red can be used to visualize lysosomal proteolysis and localization in acidified

compartments of macroautophagy-targeted GFP. In uninfected lung epithelial cells, few yellow autophagosomes but a high number of mRFP-positive autolysosomes could be detected after transient transfection of mRFP-GFP-Atg8/LC3 (Figure 2D). In contrast, influenza virus infection led to the accumulation of mRFP and GFP double-positive vesicles, especially in the perinuclear region, suggesting impaired autophagosome fusion with lysosomes. These data suggest that influenza virus infection inhibits fusion of autophagosomes with acidified LAMP1$^+$ lysosomes and thereby prevents degradation of macroautophagy substrates.

Influenza Virus-Infected Cells Accumulate Small Autophagosomes with High Mobility and Immobile Large Perinuclear Autophagosomes

In order to investigate if the block of autophagosome fusion with lysosomes in influenza virus-infected cells could result from impaired autophagosome mobility, we observed GFP-Atg8/LC3-transfected A549 lung epithelial cells by live cell imaging. Most influenza-infected cells contained numerous small autophagosomes in addition to one large GFP-LC3$^+$ perinuclear vesicle of $\geq$5 μm diameter, whereas uninfected cells contained a smaller number of evenly distributed, small-to-medium size autophagosomes (Figure 3A). The larger autophagosomes ($\geq$1 μm) in both uninfected and infected cells moved only slowly; the very large perinuclear autophagosome, which accumulated upon influenza virus infection, appeared almost immobile when followed over a period of 10 min (Figure 3A). In uninfected cells, smaller autophagosomes (<1 μm) moved slightly more rapidly than large autophagosomes and therefore could be seen to move slowly when their tracks were recorded over a period of 30 s (average speed = 0.1 μm/s) (Figure 3B, left). Strikingly, small autophagosomes in influenza-infected cells moved rapidly throughout the cytosol (Figure 3B and Movie S1). The movement seemed to be random and nondirectional, since vesicles moved toward and away from the central perinuclear region containing immobile large autophagosomes. The average speed of autophagosomes in infected cells was about 0.3 μm/s and therefore significantly elevated compared to autophagosomes in uninfected cells. These findings suggest that the block in autophagosome fusion with lysosomes is not due to impaired autophagosome mobility.

In addition to this kinetic description of the autophagosome populations in influenza virus-infected cells, we analyzed the ultrastructural features of the large perinuclear GFP-Atg8/LC3$^+$ vesicles. We analyzed influenza virus-infected human lung epithelial cells by electron microscopy in order to distinguish if these large GFP-Atg8/LC3-positive structures are autophagosomes of very large size or clusters of small autophagosomes. This also allowed us to look at the autophagosome content/composition at the ultrastructural level. In uninfected cells, a few small (0.5–1 μm) autophagosomes or autolysosomes containing internal lipid vesicles and electron-dense material could be observed (Figure 3C, top row, black arrows). In contrast, 24 hr after influenza infection, most cells contained extremely large autophagosomes (up to 7 μm) that sometimes even reached the size of the nucleus (Figure 3C, bottom row, black arrows). The giant autophagosomes contained electron-dense, amorphous material and did not seem to contain large amounts of other organelles, such as mitochondria or rough ER, which we could readily identify in the cytoplasm (Figure 3C). Our ultrastructural analysis of influenza-infected cells confirms that autophagosome numbers are strongly increased after influenza infection. Furthermore, it suggests that at least some of the large GFP-LC3-positive structures observed in fluorescence microscopy represent one unusually large autophagosome that might originate from the fusion of smaller autophagosomes.

M2 Protein of Influenza A Virus Is Sufficient to Block Autophagosome Degradation

In order to investigate how influenza A virus causes this dramatic change in autophagic activity of infected cells, we transiently transfected GFP-Atg8/LC3-positive A549 cells with expression plasmids encoding for the influenza A virus proteins PB2, NP, NS1, M1, M2, and HA. Twenty-four hours after transfection, we observed that only M2-transfected cells showed a strong accumulation of GFP-Atg8/LC3 vesicles by immunofluorescence microscopy analysis (Figure 4A), while the introduction of the other influenza A virus proteins did not result in autophagosome accumulation. The increased autophagosome number upon M2 expression could also be observed by western blot analysis as an accumulation of lipidated Atg8/LC3-II (Figure 4B). In order to compare transfection levels of influenza A proteins, we used FLAG-tagged constructs (Figure 4B). Although the FLAG tag can interfere with protein function, it did not cause autophagosome accumulation when coupled to NP and allowed autophagosome stabilization by M2. M2-mediated autophagosome accumulation was also observed in different human and mouse cell types, 293T human kidney epithelial cells, MDAMC human breast carcinoma cells, mouse embryonic fibroblasts (MEFs), and human melanoma cell lines (data not shown). In order to confirm that M2 expression also recapitulated the block of autophagosome fusion with lysosomes as observed during live influenza virus infection, we investigated autophagosome acidification and GFP degradation/quenching of the mRFP-GFP-Atg8/LC3 reporter construct in M2-transfected cells. Indeed, no overlay between autophagosomes and LysoTracker staining was observed in M2-transfected A549 cells (data not shown). Moreover, coexpression of M2 and mRFP-GFP-LC3 tandem construct led to the accumulation of mRFP and GFP double-positive vesicles, especially in the perinuclear region, suggesting impaired autophagosome fusion with lysosomes (data not shown). This observation was not the consequence of a general defect in the fusion with lysosomes, because we observed that fusion of fluorescent Sepharose beads containing phagosomes with lysosomes was intact in influenza A virus-infected and in M2-transfected cells (data not shown). These data indicate that M2 transfection recapitulates the macroautophagy block observed after influenza A virus infection.

During our immune fluorescence microscopy analysis, we noted that M2 staining localized to the cell membrane and to perinuclear autophagosomes (Figure 4A). We therefore performed a detailed colocalization analysis of GFP-LC3 and M2 in infected A549 cells (Figure 4C). We found a significant partial colocalization of these two proteins with a Pearson coefficient of 0.7, as depicted in the scatter plot (Figure 4C, lower panel) showing the pixel distribution of the two corresponding channels (number of colocalized voxels: 63,619). This example is

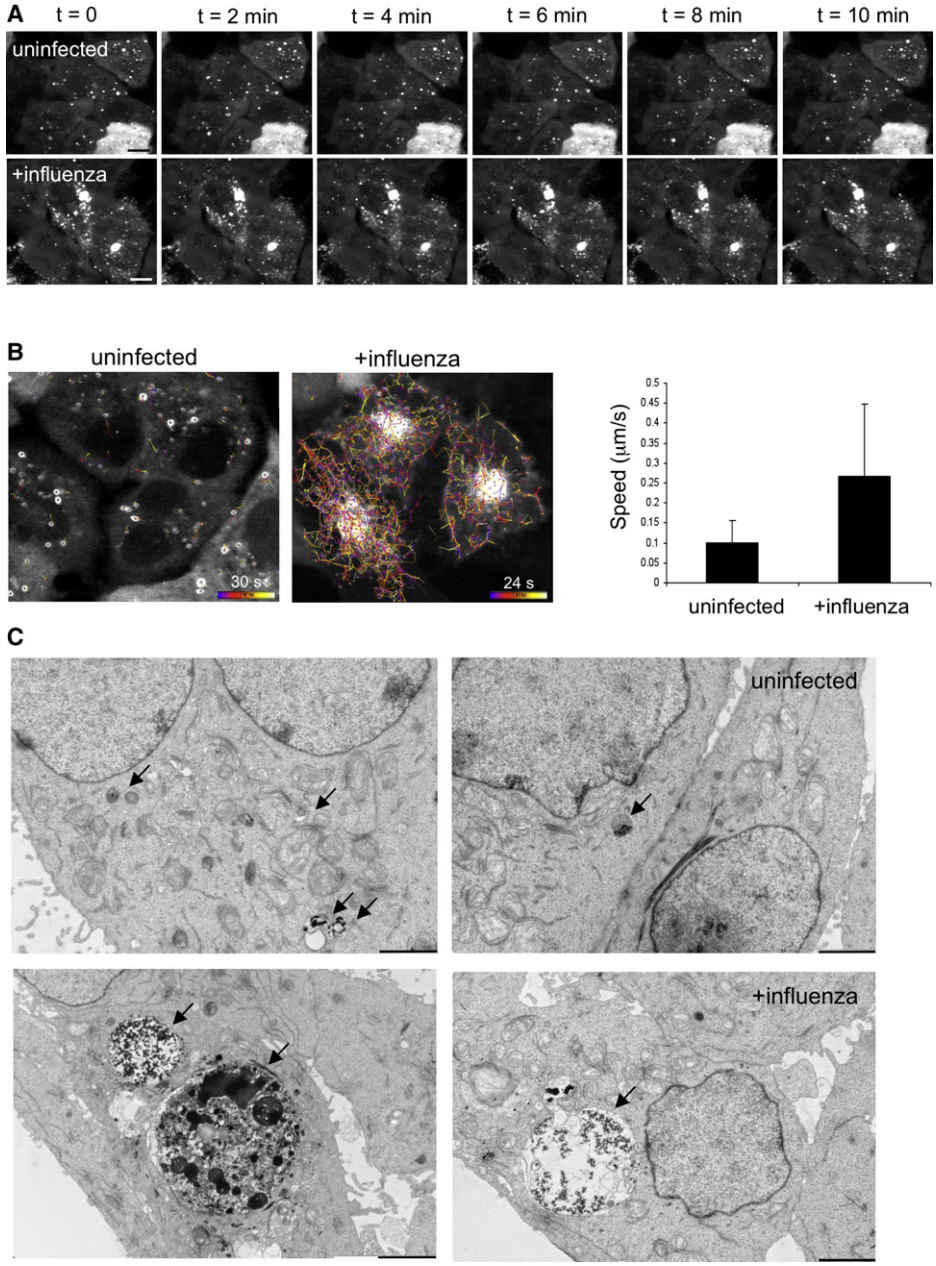

Figure 3. Mobility and Ultrastructure of Autophagosomes in Influenza A Virus-Infected Cells

(A) Live cell imaging of GFP-Atg8/LC3-transfected A549 human lung epithelial cells was performed to analyze autophagosome mobility. Still images of uninfected and influenza A virus-infected cells taken at the indicated time points of live cell imaging document the immobility of the accumulated large perinuclear autophagosomes.

(B) Autophagosome tracking in uninfected and influenza A-infected cells. Left: vesicle tracks are displayed as color-coded tracks, indicating the distance traveled by one vesicle during the indicated observation period (t = 0 in blue, t = endpoint in white). Right: average speed of autophagosomes was determined in three independent fields and summarized. One of three experiments is shown. Error bars indicate SD.

(C) Electron micrographs of uninfected and influenza A virus-infected A549 human lung epithelial cells. Small autophagic structures (black arrows, upper row) were detected in uninfected cells, whereas large autophagic structures (black arrows, lower row) were visible in infected cells. Scale bar: 2 μm. One of three experiments is shown.

representative of 36 cells that were analyzed. Overall, a Pearson coefficient of 0.6 was reached, and 42% of autophagosomes contained 12% of M2 in influenza A virus-infected cells.

In order to further support this M2 localization to autophagosomes, we performed cell fractionation and density gradient centrifugation to enrich autophagosomes from influenza A virus-infected cells. The autophagosome distribution in these density fractions was then determined by characterizing the enrichment of the Atg8 homologs LC3 (MAP1LC3B) and Gate16 (GABARAPL2); of Rab7, involved in autophagosome

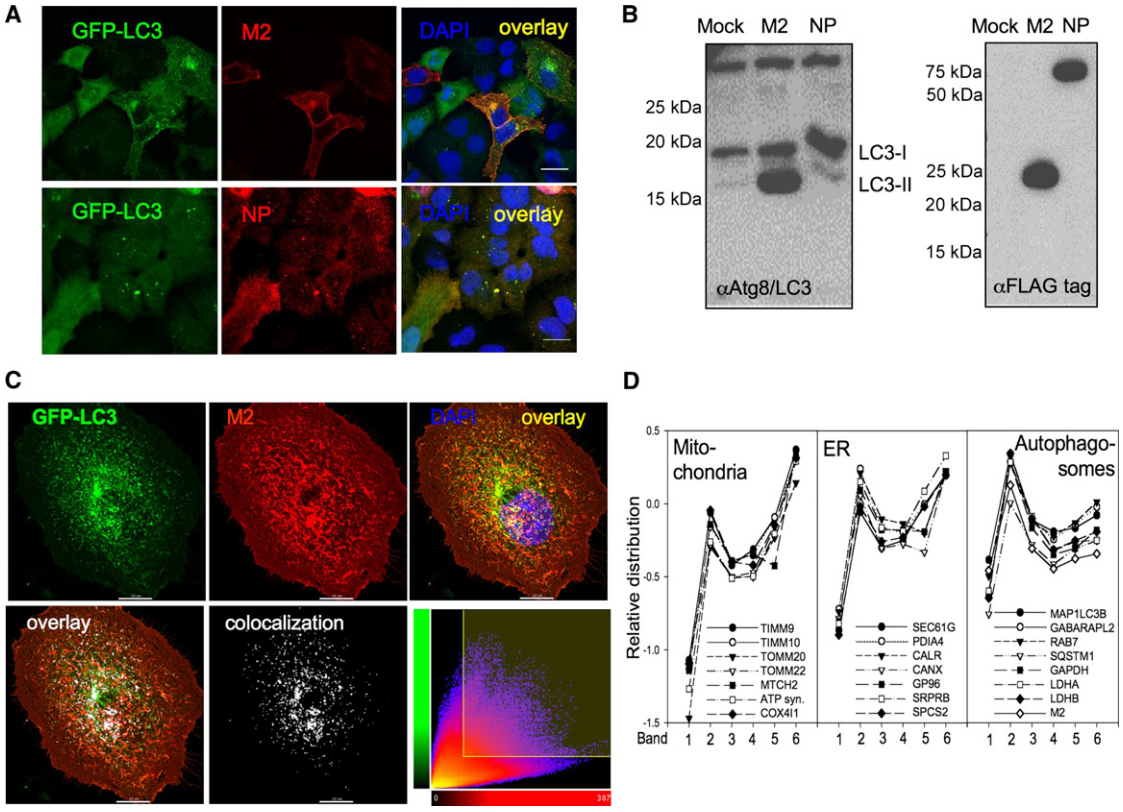

Figure 4. Influenza A Virus M2 Blocks Autophagosome Fusion with Lysosomes

(A) GFP-Atg8/LC3-transfected A549 human lung epithelial cells were transfected with expression plasmids encoding either FLAG-tagged M2 or NP of influenza A/WSN/33 virus. Twenty-four hours after transfection, GFP-ATG8/LC3-positive autophagosome accumulation was analyzed by fluorescence microscopy. Influenza M2-specific antibodies were used for M2 detection and an anti-FLAG antibody for NP detection. Scale bar: 80 μm. One of three experiments is shown.

(B) Left: western blot analysis of lipidated endogenous Atg8/LC3-II accumulation in A549 cells transfected with M2 or NP. Right: western blot analysis of M2 and NP expression in transfected cells, using anti-FLAG-tag staining. One of three experiments is shown.

(C) Colocalization analysis of M2 (red fluorescence) and GFP-LC3 (green fluorescence) in infected A549 cells: serial optical sections (0.2 μm; 40 sections) were acquired, and images were then deconvoluted using Huygens software. Pearson coefficients were calculated using the Imaris 6.3.0 software. White fluorescence represents colocalization. Scale bar: 10 μm. One representative of 36 analyzed cells is shown.

(D) Mass spectrometric analysis of density gradient fractions (1–6) of influenza A virus-infected A549 cells content upon influenza infection in A549 cells. Cell organelle marker protein distribution in these fractions was determined by mass spectrometric sequencing of protein fragments. Influenza A virus M2 distribution follows the distribution of autophagosome marker protein (right panel) but not the distribution pattern of mitochondria and endoplasmic reticulum (ER) proteins. One of four experiments is shown.

fusion with lysosomes (Jäger et al., 2004); and of the classical macroautophagy substrates p62/SQSTM1 (Komatsu et al., 2007), glyceraldehydephosphate dehydrogenase (GAPDH) (Fengsrud et al., 2000), and lactate dehydrogenase A/B (LDHA/B) (Stromhaug et al., 1998). The distribution of these proteins was determined by peptide fragment analysis via mass spectrometry (Kristensen et al., 2008). This analysis revealed that influenza A virus M2 enrichment in density gradient fractions of infected A549 cells followed the profile of autophagosome markers, but not mitochondrial and endoplasmic reticulum proteins (Figure 4D). These findings suggest that M2 accumulates in regular autophagosomes and prevents their fusion with lysosomes.

M2 Is Necessary for Autophagosome Accumulation during Influenza Virus Infection

In order to demonstrate that M2 is necessary for the block of autophagosome degradation by influenza A virus infection, we used two strategies. In a first set of experiments, we used M2-specific RNA interference, and in a second set of experiments, we used an M2 knockout virus.

Silencing of M2 protein expression during influenza A virus infection significantly decreased autophagosome accumulation in infected cells (Figure 5A). Indeed, downregulation of M2 by RNA interference reverted the phenotype of infected cells from containing perinuclear autophagosome accumulations to homogenous GFP-Atg8/LC3 distribution. This difference was statistically significant ($p < 0.001$) (Figure 5B). Loss of M2 by this treatment did, however, not prevent infection by influenza A virus, because NP expression was similar in control siRNA or M2-specific siRNA-treated cells (Figure 5A). This loss of function by M2 silencing was also observed in western blot analysis. Atg8/LC3-II upregulation during influenza A virus infection was significantly decreased upon M2-specific RNA interference (Figure 5C). To further confirm this finding, we constructed an M2 knockout virus on the A/PR8/34 influenza strain background

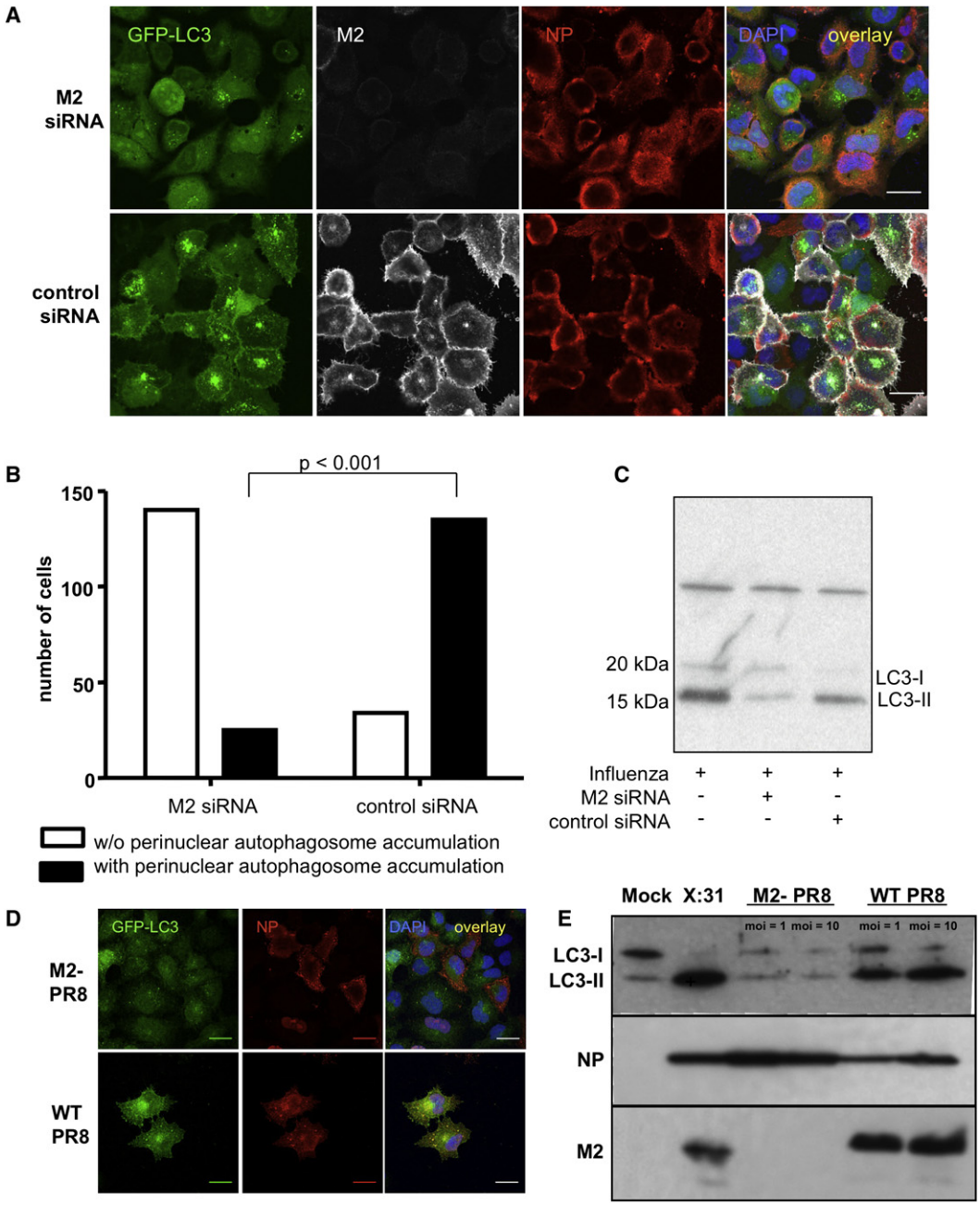

Figure 5. Loss of Influenza A Virus M2 Expression during Infection Prevents Autophagosome Accumulation

(A) GFP-Atg8/LC3-transfected A549 cells were transfected with M2-specific siRNA or a control siRNA and analyzed by fluorescence microscopy 24 hr after infection. In order to monitor influenza A virus infection and M2 expression, costaining for NP and M2 was performed. Scale bar: 30 μm. One of three experiments is shown.

(B) Summary of perinuclear autophagosome accumulation in influenza A virus-infected cells with and without M2-specific RNA silencing of three independent experiments. In each experiment, at least 150 cells were analyzed per condition. Statistical analysis was performed by applying Pearson's chi-square test.

(C) Western blot analysis of lipidated Atg8/LC3-II accumulation in influenza-infected A549 cells transfected with M2 siRNA or control siRNA. One of three experiments is shown.

(D) GFP-Atg8/LC3-transfected A549 cells at 24 hr after infection with M2-deficient (M2− PR8) or wild-type influenza A virus (WT PR8). Infection was visualized by staining for NP. Scale bar: 100 μm.

(E) Western blot analysis of Atg8/LC3-II, M2, and NP expression in influenza A virus-infected A549 cells using the two recombinant influenza A viruses (M2− PR8 and WT PR8) at mois of 1 and 10 and influenza A/X:31 virus as a control. One of five experiments is shown.

by reverse genetics. This strain background was chosen since it can perform only single-round replications in cell culture and therefore allows the analysis of cell biological effects of M2 loss without confounding effects due to blocked secondary infections. A549 cells infected with the M2-deficient virus did not show any accumulation of autophagosomes, as depicted by the GFP-Atg8/LC3 fluorescence analysis (Figure 5D). We also could not detect any Atg8/LC3-II accumulation by western blot analysis at 24 hr after infection with two different concentrations of M2 knockout virus (moi = 1 and moi = 10) (Figure 5E), while wild-type influenza A/PR8/34 virus produced with the same reverse genetics approach was capable to arrest autophagosome degradation. This difference was not due to a diminished infectivity of the M2-deficient virus, as documented by NP expression (immunofluorescence and western blot analysis [Figures 5D and 5E]). These data suggest that M2 protein is sufficient and necessary to inhibit fusion of autophagosomes with the lysosomal compartment and thereby prevents degradation of macroautophagy substrates during influenza A virus infection.

The Proton Channel Activity of M2 Is Not Involved in Blocking Autophagosome Degradation

The major function of M2 is its activity as selective proton channel during viral entry. Therefore, we hypothesized that M2 localization in the autophagosomal membranes could prevent the acidification of these vesicles and thereby inhibit their efficient fusion with lysosomes (Yamamoto et al., 1998). We first used the antiviral drug amantadine hydrochloride (AMA), an aminoadamantane known to inhibit the proton channel activity of M2 (Hay et al., 1985). This inhibitor was unable to prevent autophagosome accumulation in M2-transfected or influenza A virus-infected cells (Figure 6A). In order to confirm that viral proton channel activity alone was not sufficient for autophagosome accumulation, we tested influenza B virus infection. Influenza B virus' proton channel BM2 facilitates influenza B virus acidification during its cellular entry (Mould et al., 2003). The homology between M2 of influenza A virus and the BM2 protein of influenza B virus is, however, restricted to the HXXXW motif of the membrane-spanning residues, known to be critical for the proton channel activity (Ma et al., 2008). Surprisingly, influenza B infection did not result in autophagosome accumulation (Figure 6B). Moreover, mutating the H37 of M2 to glycine ($M2_{H37G}$), which abolishes proton channel activity (Stouffer et al., 2008), did not decrease lipidated Atg8/LC3-II accumulation in M2-transfected cells (Figure 6C). These data suggest that M2's proton channel activity is not involved in blocking autophagosome fusion with lysosomes.

We next investigated if the cytoplasmic domain of M2 was involved in autophagosome accumulation. We constructed a truncated form of M2, encoding for only the first 60 amino acids ($M2_{1–60}$). $M2_{1–60}$ transfection was still able to cause accumulation of lipidated Atg8/LC3-II (Figure 6C). We conclude from these data that the C-terminal cytoplasmic domain of M2 is not involved in autophagosome accumulation during influenza A virus infection.

Finally, in order to get a first insight into how M2 blocks autophagosome fusion with lysosomes, we analyzed if it could interact with the molecular machinery of macroautophagy. We performed immunoprecipitations of M2 to identify associated Atg proteins. We identified Atg6/Beclin-1 in M2 immunoprecipitates from influenza A virus-infected A549 cells. Similarly, M2 coimmunoprecipitated with Atg6/Beclin-1 from infected cells (Figure 6D). Furthermore, the N-terminal 60 amino acids of M2 were able to interact with Beclin-1 (Figure 6E). $M2_{1–60}$ and full-length M2 were coimmunoprecipitated with Atg6/Beclin-1 to a similar degree. These results give a first indication that $M2_{1–60}$ might interfere with the Atg6/Beclin-1- and UVRAG-containing PI3K complex, which has been recently described to facilitate autophagosome fusion with lysosomes (Matsunaga et al., 2009; Zhong et al., 2009; Itakura et al., 2008).

Thus, M2 of influenza A virus blocks autolysosome formation with its N-terminal 60 amino acids, independently of its proton channel function, possibly through interfering with the Atg6/Beclin-1- and UVRAG-containing PI3K complex.

Macroautophagy-Deficient Cells Are More Susceptible to Apoptosis upon Influenza Infection

In order to understand the functional relevance of macroautophagy inhibition upon influenza A virus infection, we used wild-type and macroautophagy-deficient MEFs. Loss of macroautophagy was achieved by knockout of the essential macroautophagy gene *atg5* (Kuma et al., 2004). Although wild-type and $atg5^{-/-}$ MEFs were similarly susceptible to apoptosis as measured by annexin V and 7-AAD staining in flow cytometry, influenza A virus infection induced significantly more cell death in macroautophagy-deficient MEFs across a broad range of different infectious doses (Figure 7A). Moreover, this susceptibility to apoptosis of $atg5^{-/-}$ MEFs was observed at several time points (6, 12, and 24 hr) after influenza A virus infection (Figure 7B). Across the different infectious doses and infection time points, influenza A-infected $atg5^{-/-}$ MEFs consistently contained up to 4-fold more apoptotic and secondary necrotic cells than infected wild-type MEFs (paired t test, $p = 0.005$). The difference in apoptosis was most pronounced 12 hr after infection and at an infectious viral dose of 120 HAU/10^6 cells. Thus, loss of autophagosome formation compromises the survival of influenza-infected cells. Furthermore, loss of the M2 block of autophagosome degradation resulted in increased survival of M2 knockout influenza A virus-infected cells (Figures 7C and 7D). The cell death was analyzed 24 hr after the infection of A549 lung epithelial cells with M2-deficient and wild-type virus. Therefore, allowing completion of macroautophagy by lifting the M2-mediated block of autophagosome fusion with lysosomes enhances survival of influenza-infected cells. These data suggest that macroautophagy serves as a survival pathway in influenza-infected cells, since its deficiency leads to enhanced apoptosis, and restoring completion of macroautophagy leads to decreased apoptosis.

Macroautophagy Deficiency Enhances Viral Protein Release but Not Viral Replication

In order to investigate if this enhanced cell death of macroautophagy-deficient cells after influenza A virus infection affects virus release, we performed HA-specific ELISA assays with the supernatants of infected $atg5^{+/+}$ and $atg5^{-/-}$ MEFs. We detected increased viral protein release from infected macroautophagy-deficient cells (Figure S2A). Four times more HA was released from infected Atg5-deficient MEFs than from infected wild-type cells. Furthermore, the viral protein content was higher in

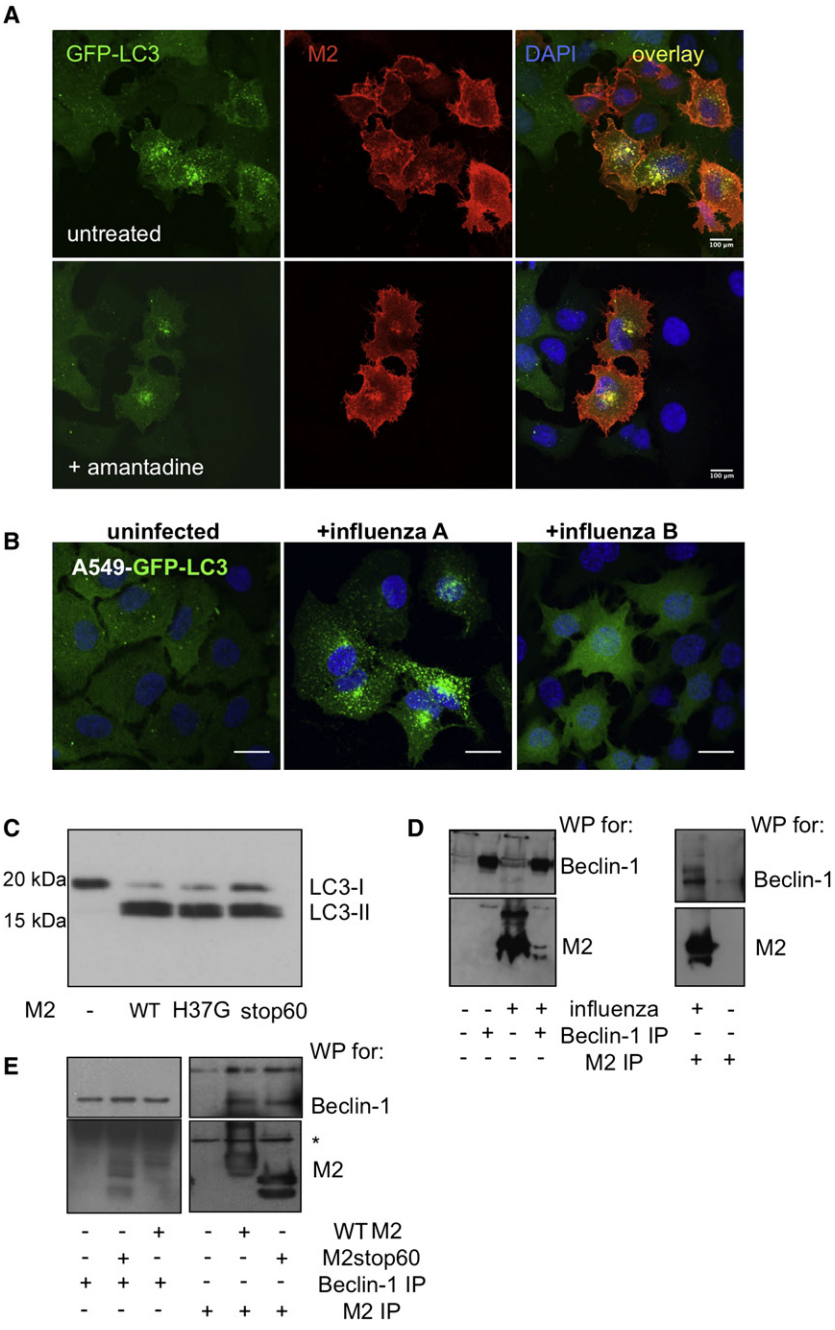

Figure 6. The Proton Channel Function of M2 Is Not Involved in Autophagosome Accumulation

(A) GFP-Atg8/LC3-transfected A549 human lung epithelial cells were infected with influenza A virus and incubated 1 hr later with and without amantadine at a concentration of 50 μM. Cells were stained with M2 antibody and analyzed for GFP-Atg8/LC3-positive autophagosome accumulation by fluorescence microscopy. Nuclear DNA was stained with DAPI. Scale bar: 100 μm. Representative images of one of three experiments are shown.

(B) GFP-Atg8/LC3-transfected A549 cells were infected with influenza A or B and analyzed by fluorescence microscopy for autophagosome accumulation. DAPI was used to stain nuclear DNA. Scale bar: 100 μm. One of three experiments is shown.

(C) A549 cells were transiently transfected with M2 wild-type and M2 mutants (M2 H37G and M2 stop60) encoding plasmids. Twenty-four hours after transfection, Atg8/LC3-II accumulation was analyzed by western blot analysis. One of three experiments is shown.

(D) A549 cells were infected with X:31 virus; 24 hr later, cell lysates from infected and noninfected cells were immunoprecipitated using Atg6/Beclin-1-specific (left) or M2-specific antibodies (right). Western blotting was performed for Atg6/Beclin-1 and influenza A virus M2 detection. One of three experiments is shown.

(E) A549 cells were transfected with full-length (WT) or the 60 N-terminal amino acids of M2 (stop60). Transfected or nontransfected cells were immunoprecipitated using Atg6/Beclin-1- or M2-specific antibodies (Atg6/Beclin-1 IP, left panel; M2 IP, right panel). Western blotting was performed for Atg6/Beclin-1 (top) and M2 (bottom) detection. * indicates immunoglobulin light chain of the antibodies used for immunoprecipitation. One of three experiments is shown.

infected macroautophagy-competent than in macroautophagy-deficient cells (Figure S2B). Similarly, more viral RNA was retained in Atg5-positive than -negative cells after influenza A virus infection (7.94-fold ± 2.68; p = 0.0005). These values were normalized to GAPDH (Figure S2C, left); these data suggest that macroautophagy-competent cells retain more viral protein and RNA within influenza A virus-infected cells.

However, we did not detect higher viral titers in the supernatants of macroautophagy-competent cells after influenza A virus infection (Figure S2D). In these experiments, influenza A virus titers were determined by MDCK plaque assay. No significant differences were detected in virus infectivity from supernatants collected from *atg5*$^{+/+}$ and *atg5*$^{-/-}$ MEFs. Overall, these data suggest that macroautophagy-competent cells accumulate more viral RNA and viral proteins than macroautophagy-deficient cells, but this does not result in higher infectious virus release.

DISCUSSION

Our study characterizes inhibition of macroautophagy by influenza A virus at the checkpoint of autophagosome fusion with lysosomes. We identify M2 as the viral protein mediating this block in autophagosome degradation and document that macroautophagy downmodulation leads to enhanced virus-induced cell death of infected cells and elevated viral antigen release.

However, influenza A virus is not the first pathogen that has been described to interfere with macroautophagy. Indeed, as early as 1965, Sam Dales and colleagues documented that poliovirus infection leads to the accumulation of double-membrane coated vesicles (Dales et al., 1965). Later, it was reported that the formation of these membrane compartments depends on some components of the macroautophagic machinery and is required for efficient viral replication (Jackson et al.,

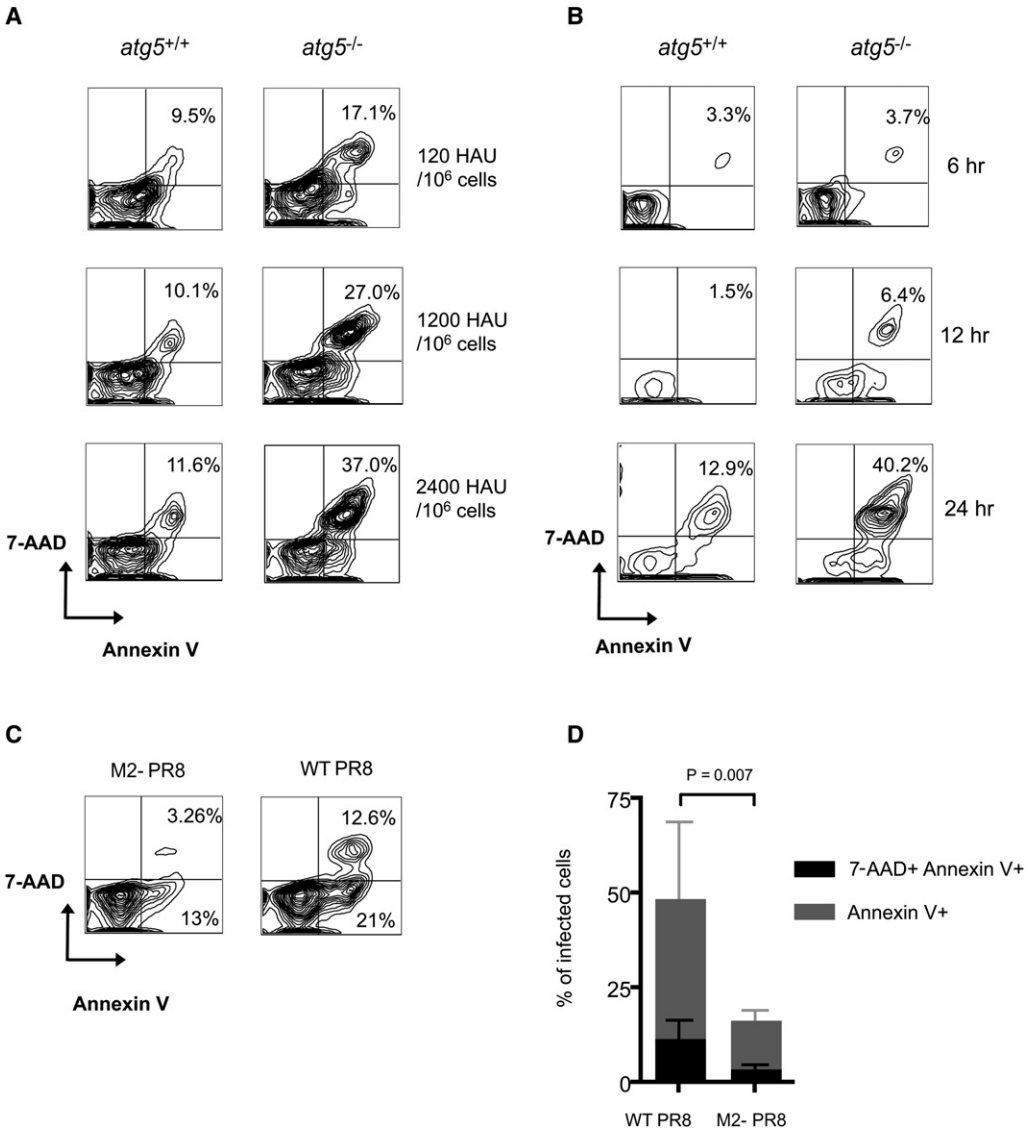

Figure 7. Macroautophagy Inhibition Enhances Cell Death after Influenza A Virus Infection

(A) Wild-type (*atg5*$^{+/+}$) and macroautophagy-deficient (*atg5*$^{-/-}$) MEFs were infected with the indicated doses of influenza A virus (HA units [HAU] per 10^6 cells) and analyzed 24 hr later by flow cytometry. Staining for M2, 7-AAD, and annexin V was performed. Cells were gated on M2-positive cells, and apoptosis (annexin V-positive) and secondary necrosis (annexin V- and 7-AAD-positive) cells were quantified. The percentage of double-positive cells (annexin V- and 7-AAD-positive) is significantly higher in *atg5*$^{-/-}$ cells (paired t test, p = 0.005). One of five experiments is shown.

(B) Cell death induction was analyzed as in (A), but with one constant influenza A virus infection dose (1200 HAU/10^6 cells) at the indicated time points. One of three experiments is shown.

(C) A549 cells were infected with the M2-deficient or the wild-type recombinant virus at an moi of 1, and cell death was analyzed at 24 hr after infection. Cells were gated on infected cells (anti-H1N1 FITC), and apoptosis (annexin V-positive) and secondary necrosis (annexin V- and 7-AAD-positive) cells were quantified.

(D) Composite data on five independent experiments comparing apoptosis (Annexin V$^+$) and secondary necrosis (7-AAD$^+$ Annexin V$^+$) after M2-deficient (M2− PR8) and wild-type (WT PR8) influenza A virus infection of A549 cells. Error bars indicate SD.

2005). Similarly, hepatitis C virus (HCV) infection leads to the accumulation of Atg8/LC3-positive vesicles, while not affecting the turnover of classical macroautophagy substrates (Sir et al., 2008). The accumulating vesicles seem to be required for HCV replication. However, even though autophagic replication compartments of pathogens seem to be stabilized and not degraded within minutes as regular autophagosomes are, the molecular mechanism (at the level of individual proteins blocking autophagosome fusion with lysosomes) remains unclear (Münz, 2009). In contrast to this second checkpoint of macroautophagic flux, inhibition of autophagosome formation as a first checkpoint during macroautophagy has been reported and characterized in more detail for several pathogens. Herpesviruses have proven a rich source of inhibitors of macroautophagy. Members of the γ-herpesviridae, namely Kaposi's sarcoma-associated herpesvirus (KSHV) and mouse herpesvirus 68 (MHV-68), have been

demonstrated to encode Bcl-2 homologs that inhibit autophagosome initiation via their binding to Atg6/Beclin-1, a component of the class III PI3K complexes that are required for macroautophagy (Ku et al., 2008; Pattingre et al., 2005; Sinha et al., 2008). Similarly, the α-herpesvirus HSV-1 encodes ICP34.5, which also contains an Atg6/Beclin-1-interacting domain, which inhibits macroautophagy (Orvedahl et al., 2007). Interestingly, HSV-1 with an ICP34.5 protein deficient in this domain is attenuated in its neurovirulence in mice. Consistent with this role of macroautophagy for resistance to HSV infection in vivo is that Sindbis virus, transgenic for Atg6/Beclin-1 and thereby enhancing macroautophagy upon infection, is attenuated in mice (Liang et al., 1998). While our study was being prepared for publication, influenza A virus was also reported to affect autophagosome formation to enhance its replication (Zhou et al., 2009). While we cannot exclude that influenza A virus might upregulate macroautophagy via innate immune recognition by PAMP receptors in certain cell types (Delgado et al., 2008), we could only identify one viral protein, namely M2, that blocks autophagosome degradation, and this was also the main mechanism of autophagosome accumulation in human lung epithelial cells after infection with a variety of influenza A virus strains. Interestingly, M2 might also target Atg6/Beclin-1 for this function, possibly interfering with the Atg6/Beclin-1- and UVRAG-containing PI3K complex, which was recently characterized to support autophagosome fusion with lysosomes (Matsunaga et al., 2009; Zhong et al., 2009; Itakura et al., 2008). Therefore, pathogens target macroautophagy at two checkpoints, during autophagosome formation and during autophagosome fusion with lysosomes, and we have characterized a specific viral protein that blocks autophagosome degradation.

Apart from mediating immunity, as has been demonstrated for other pathogens, we demonstrate that macroautophagy can also influence the death of the pathogen's host cell. In addition to regulation of the prosurvival pathway of macroautophagy by influenza A virus, several viruses influence apoptosis of infected cells (Galluzzi et al., 2008). Although one would intuitively assume that it is in the virus' interest to prolong the life of infected cells in order to maximize viral replication, pro- and antiapoptotic mechanisms are employed by viruses to nearly the same extent (Galluzzi et al., 2008). While more antiapoptotic proteins have been identified in DNA viruses, like Bcl-2 homologs of herpesviruses, RNA viruses encode more proapoptotic factors. Among the most prominent pathogens that trigger apoptosis are the RNA viruses HIV and influenza. Influenza A virus encodes the proapoptotic protein PB1-F2 (Chen et al., 2001). It inserts into the mitochondrial membrane (Gibbs et al., 2003), causing pores in lipid bilayers (Chanturiya et al., 2004), and also directly interacts with ANT and VDAC (Zamarin et al., 2005). Although it is not entirely clear if PB1-F2 causes mitochondrial membrane permeabilization by regulation of ANT and VDAC or its direct pore-forming capacity, this proapoptotic function of influenza A virus is required for pathogenesis in mice (Zamarin et al., 2006). Furthermore, PB1-F2 is in part responsible for the increased pathogenesis of the H5N1 "bird flu" and the 1918 "Spanish flu" (McAuley et al., 2007; Conenello et al., 2007). Indeed, only a single amino acid mutation was responsible for the increased pathogenicity of PB1-F2 of these highly virulent influenza A strains (Conenello et al., 2007). These studies suggest that RNA viruses like influenza induce apoptosis and thereby regulate the cell death of their host cells.

Even though proapoptotic proteins have now been identified from many pathogens, and we show in this study that influenza inhibits the prosurvival pathway of macroautophagy, the functional benefit of enhanced host cell death during infection still remains largely unclear. We propose three possible advantages of macroautophagy inhibition for influenza A virus. First, depletion of immune system cells and lung epithelial cells by apoptosis could facilitate influenza A virus infection by limiting virus-specific immune responses and compromising the lung barrier function. Within the cells of the immune system, macrophages have been found to be especially sensitive to influenza A virus-induced cell death (Bender et al., 1998), and highly pathogenic influenza virus strains were superior in lung lesion induction and dendritic cell depletion early during influenza A virus infection of macaques (Baskin et al., 2009). Second, influenza A virus-induced apoptosis has been demonstrated to limit proinflammatory cytokine production (Brydon et al., 2003). In good agreement, we find that viral RNA, which can be recognized as a PAMP to trigger inflammatory cytokine responses, is more readily retained in macroautophagy-competent cells after influenza infection (Figure S2). Therefore, induction of apoptotic cell death by influenza A virus in macroautophagy-competent cells could limit the immunogenicity of viral infection. Along these lines, it has been suggested that apoptotic bodies are less immunogenic than necrotic cell debris (Sauter et al., 2000). Moreover, ATP production by macroautophagy seems required to expose phosphatidylserine on apoptotic bodies for efficient engulfment by phagocytes and for the production of lysophosphatidylcholine to attract macrophages (Qu et al., 2007). Third, we demonstrate that macroautophagy-competent cells retain more virus-derived antigens after influenza infection. The enhanced viral antigen release by macroautophagy-deficient cells (Figure S2) could increase the antigenicity of influenza virus infection, which might be avoided by trapping of viral antigens in autophagosomes and preventing their degradation for direct presentation on MHC molecules via M2. Therefore, influenza A virus-induced cell death by apoptosis induction and macroautophagy inhibition could eliminate immune and barrier cells that limit viral spreading and render the death of infected cells as little immunogenic as possible. Since PB1-F2 is mainly expressed during later stages of the infection cycle (Chen et al., 2001), and we observed autophagosome accumulation also only at later time points after infection ($\geq$10 hr), the virus might induce host cell death with low immunogenicity in an ordered fashion after efficient initial replication.

In summary, we have identified the influenza A virus protein M2 as an inhibitor of autophagosome fusion with lysosomes, and this inhibition seems to target, with macroautophagy, a pathway that prevents apoptosis of infected cells.

EXPERIMENTAL PROCEDURES

Cell Lines

The following epithelial cell lines were used: the human keratinocyte cell line HaCat (a gift of Rajiv Khanna; Brisbane, Australia), the human breast carcinoma cell line MDAMC (a gift from Irene Joab; Paris), the human lung epithelium cell line A549 (a gift from Thomas Moran; New York), the mouse lung epithelium cell line MLE-12 (a gift from Arnoud Didierlaurent; London), the

canine kidney epithelium cell line MDCK and the human cervix carcinoma cell line HeLa (both ATCC; Manassas, VA), and the wild-type and Atg5-deficient MEFs (a gift from Noboru Mizushima; Tokyo). All epithelial cell lines were routinely cultured in DMEM with 10% FCS (Sigma; St. Louis, MO), 2 mM glutamine, 110 μg/ml sodium pyruvate, and 2 μg/ml gentamicin, except MLE-12, which was cultured in a 50:50 mix of DMEM:Ham's F12 supplemented with 2% FCS, 5 μg/ml insulin, 10 μg/ml transferrin, 30 mM sodium selenite, 10 nM hydrocortisone, 10 nM β-estradiol, 2 mM glutamine, and 2 μg/ml gentamicin. Epithelial cell monolayers were detached by one wash in PBS/0.5 mM EDTA followed by incubation in 0.05% trypsin/0.53 mM EDTA (GIBCO; North Andover, MA). Cell lines stably expressing GFP-LC3 were generated by lentiviral infection with mois of 10–40.

Antibodies

Primary Antibodies

Anti-LC3 antiserum was generated as previously described (Schmid et al., 2007) by immunizing two rabbits with the N-terminal peptide $LC3_{1–15}$ (MPSEKTFKQRRTFEQR) conjugated to KLH carrier protein (Cocalico Biologicals; Reamstown, PA). The rat anti-FLAG antibody was a gift from Cheolho Cheong (New York).

The following antibodies specific for influenza proteins were used: two influenza M2-specific monoclonal antibodies, M2-E10 (a gift from Tom Moran, New York) and M2-Clone 14C2 (Affinity Bioreagents; Rockford, IL); an influenza MP1-specific rabbit antiserum (a gift from Ari Helenius, Zürich); an influenza NP-specific rabbit antiserum (a gift from Peter Palese, New York); and an influenza NS1-specific monoclonal antibody (a gift from Peter Palese). For human p62/SQSTM1, a specific guinea pig antiserum (C terminus-specific, American Research Products; Belmont, MA) and monoclonal antibodies against LAMP1 (clone H4A3, Southern Biotech; Birmingham, AL), against actin (clone AC-40, Sigma), and against polyubiquitinated proteins (clone FK-1, Cosmo Bio Co., Ltd.; Carlsbad, CA) were used. For Atg6/Beclin-1 detection, we used a goat anti-Atg6/Beclin-1 (Santa Cruz Biotechnology; Santa Cruz, CA) for immunoprecipitation and a rabbit polyclonal antiserum (Novus Biologicals; Littleton, CO) for western blotting.

Secondary Antibodies

For immunofluorescence microscopy, we used Rhodamine Red-X (RRX)-conjugated or Cy-3-conjugated donkey anti-mouse from Jackson Laboratory (West Grove, PA), Alexa Fluor 568-conjugated goat anti-rat, Alexa Fluor 555-conjugated donkey anti-rabbit, Alexa Fluor 647-conjugated rat anti-mouse, and Alexa Fluor 647-conjugated goat anti-mouse (all from Invitrogen).

Influenza A Virus Infection

For most experiments, influenza A virus strain X31, A/Aichi/68 (H3N2) (purified virus, purchased from Charles River Laboratories; Wilmington, MA) was used. Where indicated, influenza B/Lee/40 (from Charles River Laboratories), influenza A/PR8/34, and A/PR8/34ΔNS1 (H1N1) (García-Sastre et al., 1998) or A/WSN/33 and A/WSN/33ΔPB1F2 (H1N1) (Zamarin et al., 2005) were used. Before infection, cells were washed three times in RPMI-1640 to remove FCS and then incubated with influenza virus in a small volume of RPMI-1640 for 1 hr at 37°C (moi = 0.1–2). After 1 hr, cells were washed once in PBS and then incubated in culture medium (DMEM + 10% FCS + glutamine + gentamicin) for the indicated amount of time, usually 24 hr. For heat inactivation, virus was incubated in a 56°C water bath for 30 min and then added to cells as described above.

See Supplemental Experimental Procedures for details on flow cytometry; inhibitors, synthetic peptides, and cytokines; expression plasmids and lentiviral constructs; siRNA-mediated gene silencing; M2-deficient recombinant influenza A/PR8/34 virus generation; immunocytochemistry and confocal microscopy; live cell imaging; electron microscopy; lysate preparation, SDS-PAGE, and immunoblotting; immunoprecipitation; HA ELISA assay; quantification of viral RNA; influenza virus titration; and statistics.

SUPPLEMENTAL DATA

Supplemental Data include Supplemental Experimental Procedures, Supplemental References, two figures, and one movie and can be found online at http://www.cell.com/cell-host-microbe/supplemental/S1931-3128(09)00314-X.

ACKNOWLEDGMENTS

This research is partly supported by grants from the National Cancer Institute (R01CA108609 and R01CA101741), from the Swiss National Science Foundation, and from the Foundation for the National Institutes of Health (Grand Challenges in Global Health) to C.M. and by NIAID grants U54AI57158 and U19AI62623 and an NIAID contract to support a Center for Research on Influenza Pathogenesis (CRIP, HHSN266200700010C) to A.G.-S.

Received: April 2, 2009
Revised: June 29, 2009
Accepted: September 14, 2009
Published: October 21, 2009

REFERENCES

Baskin, C.R., Bielefeldt-Ohmann, H., Tumpey, T.M., Sabourin, P.J., Long, J.P., García-Sastre, A., Tolnay, A.E., Albrecht, R., Pyles, J.A., Olson, P.H., et al. (2009). Early and sustained innate immune response defines pathology and death in nonhuman primates infected by highly pathogenic influenza virus. Proc. Natl. Acad. Sci. USA *106*, 3455–3460.

Bender, A., Albert, M., Reddy, A., Feldman, M., Sauter, B., Kaplan, G., Hellman, W., and Bhardwaj, N. (1998). The distinctive features of influenza virus infection of dendritic cells. Immunobiology *198*, 552–567.

Bjørkøy, G., Lamark, T., Brech, A., Outzen, H., Perander, M., Overvatn, A., Stenmark, H., and Johansen, T. (2005). p62/SQSTM1 forms protein aggregates degraded by autophagy and has a protective effect on huntingtin-induced cell death. J. Cell Biol. *171*, 603–614.

Brydon, E.W., Smith, H., and Sweet, C. (2003). Influenza A virus-induced apoptosis in bronchiolar epithelial (NCI-H292) cells limits pro-inflammatory cytokine release. J. Gen. Virol. *84*, 2389–2400.

Chanturiya, A.N., Basañez, G., Schubert, U., Henklein, P., Yewdell, J.W., and Zimmerberg, J. (2004). PB1-F2, an influenza A virus-encoded proapoptotic mitochondrial protein, creates variably sized pores in planar lipid membranes. J. Virol. *78*, 6304–6312.

Chen, W., Calvo, P.A., Malide, D., Gibbs, J., Schubert, U., Bacik, I., Basta, S., O'Neill, R., Schickli, J., Palese, P., et al. (2001). A novel influenza A virus mitochondrial protein that induces cell death. Nat. Med. *7*, 1306–1312.

Ciechanover, A. (2005). Intracellular protein degradation: from a vague idea thru the lysosome and the ubiquitin-proteasome system and onto human diseases and drug targeting. Cell Death Differ. *12*, 1178–1190.

Conenello, G.M., Zamarin, D., Perrone, L.A., Tumpey, T., and Palese, P. (2007). A single mutation in the PB1-F2 of H5N1 (HK/97) and 1918 influenza A viruses contributes to increased virulence. PLoS Pathog. *3*, 1414–1421.

Dales, S., Eggers, H.J., Tamm, I., and Palade, G.E. (1965). Electron microscopic study of the formation of poliovirus. Virology *26*, 379–389.

Delgado, M.A., Elmaoued, R.A., Davis, A.S., Kyei, G., and Deretic, V. (2008). Toll-like receptors control autophagy. EMBO J. *27*, 1110–1121.

Fengsrud, M., Raiborg, C., Berg, T.O., Strømhaug, P.E., Ueno, T., Erichsen, E.S., and Seglen, P.O. (2000). Autophagosome-associated variant isoforms of cytosolic enzymes. Biochem. J. *352*, 773–781.

Fujita, N., Itoh, T., Omori, H., Fukuda, M., Noda, T., and Yoshimori, T. (2008). The Atg16L complex specifies the site of LC3 lipidation for membrane biogenesis in autophagy. Mol. Biol. Cell *19*, 2092–2100.

Galluzzi, L., Brenner, C., Morselli, E., Touat, Z., and Kroemer, G. (2008). Viral control of mitochondrial apoptosis. PLoS Pathog. *4*, e1000018.

García-Sastre, A., Egorov, A., Matassov, D., Brandt, S., Levy, D.E., Durbin, J.E., Palese, P., and Muster, T. (1998). Influenza A virus lacking the NS1 gene replicates in interferon-deficient systems. Virology *252*, 324–330.

Gibbs, J.S., Malide, D., Hornung, F., Bennink, J.R., and Yewdell, J.W. (2003). The influenza A virus PB1-F2 protein targets the inner mitochondrial membrane via a predicted basic amphipathic helix that disrupts mitochondrial function. J. Virol. *77*, 7214–7224.

Hanada, T., Noda, N.N., Satomi, Y., Ichimura, Y., Fujioka, Y., Takao, T., Inagaki, F., and Ohsumi, Y. (2007). The Atg12-Atg5 conjugate has a novel

E3-like activity for protein lipidation in autophagy. J. Biol. Chem. *282*, 37298–37302.

Hara, T., Nakamura, K., Matsui, M., Yamamoto, A., Nakahara, Y., Suzuki-Migishima, R., Yokoyama, M., Mishima, K., Saito, I., Okano, H., and Mizushima, N. (2006). Suppression of basal autophagy in neural cells causes neurodegenerative disease in mice. Nature *441*, 885–889.

Hay, A.J., Wolstenholme, A.J., Skehel, J.J., and Smith, M.H. (1985). The molecular basis of the specific anti-influenza action of amantadine. EMBO J. *4*, 3021–3024.

Itakura, E., Kishi, C., Inoue, K., and Mizushima, N. (2008). Beclin 1 forms two distinct phosphatidylinositol 3-kinase complexes with mammalian Atg14 and UVRAG. Mol. Biol. Cell *19*, 5360–5372.

Jackson, W.T., Giddings, T.H., Jr., Taylor, M.P., Mulinyawe, S., Rabinovitch, M., Kopito, R.R., and Kirkegaard, K. (2005). Subversion of cellular autophagosomal machinery by RNA viruses. PLoS Biol. *3*, e156.

Jäger, S., Bucci, C., Tanida, I., Ueno, T., Kominami, E., Saftig, P., and Eskelinen, E.L. (2004). Role for Rab7 in maturation of late autophagic vacuoles. J. Cell Sci. *117*, 4837–4848.

Kimura, S., Noda, T., and Yoshimori, T. (2007). Dissection of the autophagosome maturation process by a novel reporter protein, tandem fluorescent-tagged LC3. Autophagy *3*, 452–460.

Klionsky, D.J., Abeliovich, H., Agostinis, P., Agrawal, D.K., Aliev, G., Askew, D.S., Baba, M., Baehrecke, E.H., Bahr, B.A., Ballabio, A., et al. (2008). Guidelines for the use and interpretation of assays for monitoring autophagy in higher eukaryotes. Autophagy *4*, 151–175.

Komatsu, M., Waguri, S., Chiba, T., Murata, S., Iwata, J., Tanida, I., Ueno, T., Koike, M., Uchiyama, Y., Kominami, E., and Tanaka, K. (2006). Loss of autophagy in the central nervous system causes neurodegeneration in mice. Nature *441*, 880–884.

Komatsu, M., Waguri, S., Koike, M., Sou, Y.S., Ueno, T., Hara, T., Mizushima, N., Iwata, J., Ezaki, J., Murata, S., et al. (2007). Homeostatic levels of p62 control cytoplasmic inclusion body formation in autophagy-deficient mice. Cell *131*, 1149–1163.

Kristensen, A.R., Schandorff, S., Hoyer-Hansen, M., Nielsen, M.O., Jäättelä, M., Dengjel, J., and Andersen, J.S. (2008). Ordered organelle degradation during starvation-induced autophagy. Mol. Cell. Proteomics *7*, 2419–2428.

Ku, B., Woo, J.S., Liang, C., Lee, K.H., Hong, H.S., E, X., Kim, K.S., Jung, J.U., and Oh, B.H. (2008). Structural and biochemical bases for the inhibition of autophagy and apoptosis by viral BCL-2 of murine gamma-herpesvirus 68. PLoS Pathog. *4*, e25.

Kuma, A., Hatano, M., Matsui, M., Yamamoto, A., Nakaya, H., Yoshimori, T., Ohsumi, Y., Tokuhisa, T., and Mizushima, N. (2004). The role of autophagy during the early neonatal starvation period. Nature *432*, 1032–1036.

Liang, X.H., Kleeman, L.K., Jiang, H.H., Gordon, G., Goldman, J.E., Berry, G., Herman, B., and Levine, B. (1998). Protection against fatal Sindbis virus encephalitis by beclin, a novel Bcl-2-interacting protein. J. Virol. *72*, 8586–8596.

Ma, C., Soto, C.S., Ohigashi, Y., Taylor, A., Bournas, V., Glawe, B., Udo, M.K., Degrado, W.F., Lamb, R.A., and Pinto, L.H. (2008). Identification of the pore-lining residues of the BM2 ion channel protein of influenza B virus. J. Biol. Chem. *283*, 15921–15931.

Matsunaga, K., Saitoh, T., Tabata, K., Omori, H., Satoh, T., Kurotori, N., Maejima, I., Shirahama-Noda, K., Ichimura, T., Isobe, T., et al. (2009). Two Beclin 1-binding proteins, Atg14L and Rubicon, reciprocally regulate autophagy at different stages. Nat. Cell Biol. *11*, 385–396.

McAuley, J.L., Hornung, F., Boyd, K.L., Smith, A.M., McKeon, R., Bennink, J., Yewdell, J.W., and McCullers, J.A. (2007). Expression of the 1918 influenza A virus PB1-F2 enhances the pathogenesis of viral and secondary bacterial pneumonia. Cell Host Microbe *2*, 240–249.

Mizushima, N., and Klionsky, D.J. (2007). Protein turnover via autophagy: implications for metabolism. Annu. Rev. Nutr. *27*, 19–40.

Mould, J.A., Paterson, R.G., Takeda, M., Ohigashi, Y., Venkataraman, P., Lamb, R.A., and Pinto, L.H. (2003). Influenza B virus BM2 protein has ion channel activity that conducts protons across membranes. Dev. Cell *5*, 175–184.

Münz, C. (2009). Enhancing immunity through autophagy. Annu. Rev. Immunol. *27*, 423–429.

Ohsumi, Y. (2001). Molecular dissection of autophagy: two ubiquitin-like systems. Nat. Rev. Mol. Cell Biol. *2*, 211–216.

Orvedahl, A., Alexander, D., Tallóczy, Z., Sun, Q., Wei, Y., Zhang, W., Burns, D., Leib, D., and Levine, B. (2007). HSV-1 ICP34.5 confers neurovirulence by targeting the Beclin 1 autophagy protein. Cell Host Microbe *1*, 23–35.

Palese, P., and Shaw, M.L. (2007). Orthomyxoviridae: the viruses and their replication. In Fields Virology, D.M. Knipe and P.M. Howley, eds. (Philadelphia: Lippincott, Williams & Wilkins), pp. 1647–1689.

Pankiv, S., Clausen, T.H., Lamark, T., Brech, A., Bruun, J.A., Outzen, H., Øvervatn, A., Bjørkøy, G., and Johansen, T. (2007). p62/SQSTM1 binds directly to Atg8/LC3 to facilitate degradation of ubiquitinated protein aggregates by autophagy. J. Biol. Chem. *282*, 24131–24145.

Pattingre, S., Tassa, A., Qu, X., Garuti, R., Liang, X.H., Mizushima, N., Packer, M., Schneider, M.D., and Levine, B. (2005). Bcl-2 antiapoptotic proteins inhibit Beclin 1-dependent autophagy. Cell *122*, 927–939.

Qu, X., Zou, Z., Sun, Q., Luby-Phelps, K., Cheng, P., Hogan, R.N., Gilpin, C., and Levine, B. (2007). Autophagy gene-dependent clearance of apoptotic cells during embryonic development. Cell *128*, 931–946.

Sauter, B., Albert, M.L., Francisco, L., Larsson, M., Somersan, S., and Bhardwaj, N. (2000). Consequences of cell death: exposure to necrotic tumor cells, but not primary tissue cells or apoptotic cells, induces the maturation of immunostimulatory dendritic cells. J. Exp. Med. *191*, 423–434.

Schmid, D., and Münz, C. (2007). Innate and adaptive immunity through autophagy. Immunity *26*, 11–21.

Schmid, D., Pypaert, M., and Münz, C. (2007). MHC class II antigen loading compartments continuously receive input from autophagosomes. Immunity *26*, 79–92.

Sinha, S., Colbert, C.L., Becker, N., Wei, Y., and Levine, B. (2008). Molecular basis of the regulation of Beclin 1-dependent autophagy by the gamma-herpesvirus 68 Bcl-2 homolog M11. Autophagy *4*, 989–997.

Sir, D., Chen, W.L., Choi, J., Wakita, T., Yen, T.S., and Ou, J.H. (2008). Induction of incomplete autophagic response by hepatitis C virus via the unfolded protein response. Hepatology *48*, 1054–1061.

Stouffer, A.L., Acharya, R., Salom, D., Levine, A.S., Di Costanzo, L., Soto, C.S., Tereshko, V., Nanda, V., Stayrook, S., and DeGrado, W.F. (2008). Structural basis for the function and inhibition of an influenza virus proton channel. Nature *451*, 596–599.

Stromhaug, P.E., Berg, T.O., Fengsrud, M., and Seglen, P.O. (1998). Purification and characterization of autophagosomes from rat hepatocytes. Biochem. J. *335*, 217–224.

Yamamoto, A., Tagawa, Y., Yoshimori, T., Moriyama, Y., Masaki, R., and Tashiro, Y. (1998). Bafilomycin A1 prevents maturation of autophagic vacuoles by inhibiting fusion between autophagosomes and lysosomes in rat hepatoma cell line, H-4-II-E cells. Cell Struct. Funct. *23*, 33–42.

Yewdell, J., and García-Sastre, A. (2002). Influenza virus still surprises. Curr. Opin. Microbiol. *5*, 414–418.

Zamarin, D., García-Sastre, A., Xiao, X., Wang, R., and Palese, P. (2005). Influenza virus PB1-F2 protein induces cell death through mitochondrial ANT3 and VDAC1. PLoS Pathog. *1*, e4.

Zamarin, D., Ortigoza, M.B., and Palese, P. (2006). Influenza A virus PB1-F2 protein contributes to viral pathogenesis in mice. J. Virol. *80*, 7976–7983.

Zhong, Y., Wang, Q.J., Li, X., Yan, Y., Backer, J.M., Chait, B.T., Heintz, N., and Yue, Z. (2009). Distinct regulation of autophagic activity by Atg14L and Rubicon associated with Beclin 1-phosphatidylinositol-3-kinase complex. Nat. Cell Biol. *11*, 468–476.

Zhou, Z., Jiang, X., Liu, D., Fan, Z., Hu, X., Yan, J., Wang, M., and Gao, G.F. (2009). Autophagy is involved in influenza A virus replication. Autophagy *5*, 321–328.